Matrix isolation mid- and far-infrared spectra of sulfuric acid and deuterated sulfuric acid vapors

ARTICLE *in* JOURNAL OF MOLECULAR STRUCTURE · OCTOBER 1999

Impact Factor: 1.6 · DOI: 10.1016/S0022-2860(99)00209-4

4 AUTHORS, INCLUDING:

A. Loewenschuss
Hebrew University of Jerusalem
83 PUBLICATIONS **1,425** CITATIONS

ELSEVIER

Journal of Molecular Structure 509 (1999) 35–47

Journal of
MOLECULAR
STRUCTURE

www.elsevier.nl/locate/molstruc

Matrix isolation mid- and far-infrared spectra of sulfuric acid and deuterated sulfuric acid vapors ☆

A. Givan[a], L.A. Larsen[b], A. Loewenschuss[a,*], C.J. Nielsen[b]

[a]*Department of Inorganic and Analytical Chemistry, The Hebrew University of Jerusalem, Jerusalem 91904, Israel*
[b]*Department of Chemistry, University of Oslo, Blindern, N-0315 Oslo, Norway*

Received 17 February 1999; accepted 16 March 1999

Abstract

Infrared spectra of sulfuric acid and mixtures of sulfuric acid with the mono- and dideuterated species isolated in argon matrices at 5 K were obtained in the region 4000–180 cm^{-1}. The spectra were assigned in terms of C_2 symmetry and compared with the results of the ab initio calculations. Our previous mid-infrared assignment is augmented and *all* the 15 normal modes of the argon isolated H_2SO_4 monomer are now assigned for the first time. Thermodynamic properties are calculated based upon these vibrational frequencies and structural parameters. Bands attributed to the deuterated water complex species support previous assumptions in regard to bonding and structure.

Keywords: Sulfuric acid; Infrared spectroscopy; Matrix isolation; Ab initio calculations; Normal modes

1. Introduction

Sulfuric acid is an important industrial chemical. The renewed interest in its properties originates in environmental problems such as acid rain and stratospheric ozone depletion. In the troposphere, due to its large affinity towards water, it is thought to exist as hydrates ($(H_2SO_4)\cdot(H_2O)_n$, $n = 1–3$) or in aerosols [1]. In the stratosphere, where the water vapor volume fraction is only 4–5 ppm, it may also exist in the free molecular form. During our laboratory studies of the physical properties of sulfuric acid, it became evident that the spectroscopic data of sulfuric acid are incomplete, especially where the vapor phase is concerned. Vibrational spectra of the gas phase [2–6], of the liquid and aqueous solutions [7–12], as well as of crystalline H_2SO_4 have been reported [13]. Matrix isolation data are limited to the assignment of the most prominent H_2SO_4 bands appearing as by-products in the co-deposits of H_2O and SO_3 in Ne matrices [14] and from the photooxidation of H_2S in a low temperature O_2 solid [15]. Recently, we have presented a mid-IR matrix isolation study of H_2SO_4 and its complexation products with water [16], revealing, on the one hand, the existence of a variety of stable and metastable $(H_2O)_n\cdot(H_2SO_4)_m$ molecular species and, on the other, the inability of an argon matrix to stabilize any $(H_2O)_m\cdot(SO_3)_n$ complexes, the assumed intermediates in the reaction chain forming H_2SO_4 from SO_2 in the vapor phase [17–22]. This study was followed by the analysis of the infrared spectra of H_2SO_4 matrix isolated complexes with CO [23], NO, N_2O_2, and N_2 [24], HCl [25] and CO_2 [26]. The crystal structure of

☆ In honour of Professor Peter Klæboe on the occasion of his 70th birthday.

* Corresponding author. Tel.: + 972-2-658-5313; fax: + 972-2-658-5319.

E-mail address: loewena@vms.huji.ac.il (A. Loewenschuss)

0022-2860/99/$ - see front matter
PII: S0022-2860(99)00209-4

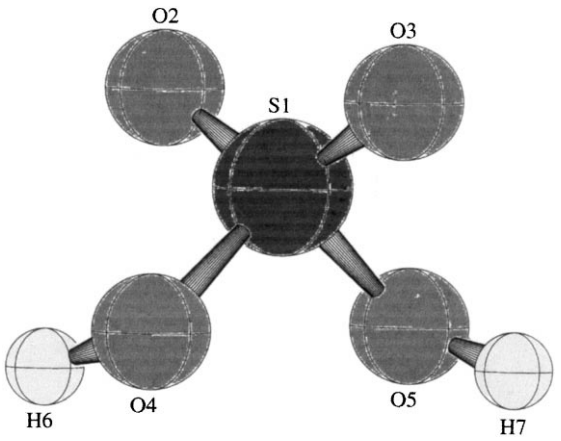

Fig. 1. H_2SO_4 molecular structure.

sulfuric acid including H-atom positions has recently been determined [27]. The stable conformer of the gaseous H_2SO_4 monomer was shown by microwave spectroscopy to be of C_2 symmetry [28], subsequently confirmed by several theoretical investigations [29–31]. In the present study the fundamental vibrational modes of $HDSO_4$ and D_2SO_4 isolated in solid argon were obtained and compared to those of H_2SO_4. The present spectral data of the deuterated species enabled us to reexamine previous [16] band assignments of the water complexes of sulfuric acid.

2. Experimental

Sulfuric acid (*p.a.*) was supplied by Prolabo, 99.5 at% deutero sulfuric acid by Fluka, and the Ar gas (5.7) by AGA. To produce the acid vapors for deposition, a drop of the acid was placed in a tube-like quartz furnace ending in a nozzle. After lengthy pumping on the furnace and cryostat, the system was cooled down, with the deposition window turned away. The furnace/nozzle was heated to ca. 35°C and the argon matrix gas dosed through a second nozzle to mix with the acid vapor effusing from the furnace prior to trapping on the cold window. The mixing ratios were estimated from pressure measurements, flow rates and the calculated partial pressure above liquid H_2SO_4 (see below). Typical compositions ranging from 1:300 to 1:1000 argon guest ratios were sprayed onto a CsI window kept at 5–15 K. Cooling was provided by an Air Products HS-4 Heliplex cryostat employing two HC-4 MK 1 compressor modules. Temperatures were controlled by a LakeShore model 330 controller, using Si diode sensors. Typical deposition times were 1–3 h depending upon sample dilution, while deposition rates were of several mmol Ar per hour. Infrared spectra were recorded on a Bruker IFS 88 FTIR spectrometer employing a DTGS detector, co-adding from 32 to 128 scans at nominal resolutions of 0.5–1 cm^{-1}.

The vapor pressure above 99 wt.% H_2SO_4 has been measured in the range 338–445 K from which one may extrapolate a value of 7×10^{-8} atm at 310 K [32]. Sulfuric acid and water form an azeotrope and in the vapor phase the acid dissociates, $H_2SO_4(g) \leftrightarrow SO_3(g) + H_2O(g)$. The equilibrium constant for this dissociation and its temperature dependence can be calculated from the thermodynamic functions of the pure components, $K_p(310) = 2.9 \times 10^{-9}$ atm [33]. Assuming equilibrium conditions above a 99 wt.% sulfuric acid and that all water vapor in the quartz oven originates from the azeotrope and the dissociation of gaseous sulfuric acid, one arrives at a vapor composition of ca. 66% $H_2SO_4(g)$, 19% $H_2O(g)$ and 15 % $SO_3(g)$ at 310 K.

3. Results and discussion

3.1. Ab initio calculations

The ab initio calculations on sulfuric acid were carried out employing the GAUSSIAN 94 program [34]. Several levels of approximation were examined and the minima on the potential surface were found by relaxing the geometry. For all calculation levels we found only one stable conformation (C_2 symmetry) where internal H-bonds are formed both to one sp^2 hybridized oxygen atom and to the oxygen atom of the other hydroxyl group. For the sake of brevity, results are only presented for the MP2/6-311++G(2d,2p) calculations—the highest calculation level used. The minimum energy conformation is presented in Fig. 1. Other results from the calculations include the internal harmonic force field (Cartesian) and infrared absorption cross sections and will be addressed later.

Table 1
Ab initio calculated structural parameters of sulfuric acid

	X-ray[a]	Microwave[b]	Ab initio
Distances (pm)			
$R_{S1=O2}$	142.6(1)	142.2(10)	142.9
R_{S1-O4}	153.7(1)	157.4(10)	160.2
R_{O4-H6}		97.0(10)	96.7
Angles (degree)			
$\alpha_{O2=S1=O3}$		123.3(10)	124.77
$\alpha_{O2=S1-O4}$		108.6(5)	108.77
$\alpha_{O2=S1-O5}$		106.4(5)	105.27
$\alpha_{O4-S1-O5}$		101.3(10)	101.73
$\alpha_{S1-O4-H6}$		108.5(5)	107.66
Dihedral angles (degree)			
$\tau_{O2=S1-O5-H7}$			164.51

[a] Crystal structure data from Ref. [27].
[b] Preferred structure from microwave data, Ref. [28].

3.2. H_2SO_4 structure and conformation

The microwave spectrum of sulfuric acid was assigned in terms of a C_2 conformation [28]. However, several lines of appreciable intensity remained unexplained and the existence of another conformation could not be ruled out. In the two older ab initio studies [29,30] the bond distances and valence angles were constrained to the values obtained in the microwave study and the torsional potential surface was calculated using the STO-3G basis set. Both studies indicated the existence of two *synclinal*, *synclinal* minima of C_2 and C_s symmetry, respectively. The barrier to interconversion was calculated as ca. 30 kJ mol^{-1} in the C_{2v} configuration (*syn*, *syn*) and the C_s form was estimated to have ca. 6 kJ mol^{-1} higher energy [30]. Our calculations, with small to medium sized basis sets and full geometry optimization, show that there is only one conformation of sulfuric acid.

The structural parameters listed in Table 1 show a very good agreement between the preferred (mixed r_S and r_O) microwave structure [28]. The crystal structure at 113 K clearly shows the effect of intermolecular hydrogen bonding involving all four oxygen atoms [27]. Apart from a 2 pm shorter S–O distance in the present calculation the structure is essentially the same as that from a recent MP2/6-31+G* calculation [31]. One notices the large deviation of the O=S=O angle from the tetrahedral value, indicative of the influence of the internal H bonding, also evidenced in the OH/OD band wave number values, as further discussed below.

3.3. Normal mode calculations

The 15 normal modes of H_2SO_4 are all infrared active and span the representation: $\Gamma_{vib} = 8a + 7b$. The ab initio calculated vibrational wave numbers invariably differ from the experimental values. Using a relatively large basis set, such as the 6-311++G (2d,2p) set, and by including electron

Table 2
Symmetry coordinates for sulfuric acid (see Fig. 1 for numbering of atoms)

a	1	O–H symmetric stretch	$S_1 = 2^{-1/2}\,(\Delta R_{46} + \Delta R_{57})$[a]
	2	S=O symmetric stretch	$S_2 = 2^{-1/2}\,(\Delta R_{12} + \Delta R_{13})$
	3	S–O–H symmetric bend	$S_3 = 2^{-1/2}\,(\Delta \alpha_{146} + \Delta \alpha_{157})$[a]
	4	S–O symmetric stretch	$S_4 = 2^{-1/2}\,(\Delta R_{14} + \Delta R_{15})$
	5	O=S=O bend	$S_5 = \Delta \alpha_{213}$
	6	O–S=O twist	$S_6 = 1/2\,(\Delta \alpha_{214} - \Delta \alpha_{215} - \Delta \alpha_{314} + \Delta \alpha_{315})$
	7	O–S=O bend	$S_7 = 1/2\,(\Delta \alpha_{214} + \Delta \alpha_{215} + \Delta \alpha_{314} + \Delta \alpha_{315})$
	8	O=S–O–H symmetric torsion	$S_8 = 2^{-1/2}\,(\Delta \tau_{2146} + \Delta \tau_{3157})$[a]
b	9	O–H antisymmetric stretch	$S_9 = 2^{-1/2}\,(\Delta R_{46} - \Delta R_{57})$[a]
	10	S=O antisymmetric stretch	$S_{10} = 2^{-1/2}\,(\Delta R_{12} - \Delta R_{13})$
	11	S–O–H antisymmetric bend	$S_{11} = 2^{-1/2}\,(\Delta \alpha_{146} - \Delta \alpha_{157})$[a]
	12	S–O antisymmetric stretch	$S_{12} = 2^{-1/2}\,(\Delta R_{14} - \Delta R_{15})$
	13	O–S=O rock	$S_{13} = 1/2\,(\Delta \alpha_{214} - \Delta \alpha_{215} + \Delta \alpha_{314} - \Delta \alpha_{315})$
	14	O=S=O wag	$S_{14} = 1/2\,(\Delta \alpha_{214} + \Delta \alpha_{215} - \Delta \alpha_{314} - \Delta \alpha_{315})$
	15	O=S–O–H antisymmetric torsion	$S_{15} = 2^{-1/2}\,(\Delta \tau_{2146} - \Delta \tau_{3157})$[a]

[a] For $HDSO_4$ the definitions are: S_1, OH stretch; S_9, OD stretch; S_3, S–O–H bend; S_{11}, S–O–D bend; S_8, O=S–O–H torsion; S_{15}, O=S–O–D torsion.

correlation through second order Møeller–Plesset perturbation in the theoretical treatment, one may expect to predict the equilibrium structure and the internal harmonic force field within a few percent of their "true" values. A normal coordinate analysis, based upon the ab initio calculated harmonic force constants, was carried out as described below to assist in assigning the observed infrared bands. First, the ab initio calculated force field was transformed from Cartesian to symmetry coordinates, derived from a suitable set of valence coordinates, Table 2. Then, a scaling of the symmetry force field was performed according to: $F_{ij}^{\text{scaled}} = F_{ij}\sqrt{\alpha_i \alpha_j}$, where F_{jj} and F_{ij}^{scaled} are the unscaled and scaled internal force fields, respectively, α_i and α_j are scale factors corresponding to internal coordinates i and j. The scale factors corresponding to symmetry coordinates involving the same class of valence coordinates were taken as identical. This leads to a significant reduction in the number of scale factors. In the present case there are six classes of valence coordinates (ΔR_{OH}, ΔR_{S-O}, $\Delta R_{S=O}$, $\Delta\alpha_{OSO}$, $\Delta\alpha_{SOH}$, $\Delta\tau_{OSOH}$) and the force field was scaled by six factors to fit the observed fundamental modes of vibration with an average relative error of ca. 0.5%. The results are included in Tables 4 and 5, as is also a normal mode description based on the potential energy distribution.

3.4. Infrared matrix isolation spectra

The infrared spectra recorded are complicated due to both the multi component composition of the vapor phase, comprising H_2SO_4, $HDSO_4$, D_2SO_4, SO_3, H_2O, HDO, and D_2O and the formation, in the matrix, of various pure and mixed dimers and higher polymers. A comparison to the simpler $H_2SO_4/SO_3/H_2O$ samples [16] is helpful in singling out the bands of the deuterated species, which are summarized and assigned in Table 3. The assigned H_2SO_4, D_2SO_4 and $HDSO_4$ fundamental frequencies are then separately collected in Table 4 (H_2SO_4, D_2SO_4) and Table 5 ($HDSO_4$) together with the previous data from the vapor phase [2–6], Ne matrix [14], O_2 matrix [15], and with the results of normal mode calculations. Spectra of the different regions are given in Figs. 2–9. In all figures, trace A is a spectrum of a sample produced from vapors over H_2SO_4, while traces B and C present spectra of the 5 K deposited and temperature cycled isotopically mixed samples, respectively, of matrix isolated vapors over deuterated sulfuric acid (referred to as "D_2SO_4"). In the following text, bandwidth values in parentheses follow the wavenumber positions.

Table 3
Mid- and far-infrared spectrum of deuterated sulfuric acid vapor species trapped in argon at 5 K (cm^{-1})

3582 (m)	OH stretch of $(H_2O)_2$/$(HDO)_2$·$(HDSO_4)$/H_2SO_4
3572.6 (m)	OH stretch of (H_2O)/(HDO)/(D_2O)·$(HDSO_4)$/H_2SO_4
3569.1 (s)	ν_1 OH stretch of $HDSO_4$
2643.2 (m)	OD stretch of $(D_2O)_2$/$(HDO)_2$/$(H_2O)_2$·$(HDSO_4)$/(D_2SO_4)
2638.5 (m)	OD stretch of (D_2O)/(HDO)/(H_2O)·$(HDSO_4)$/(D_2SO_4)
2634.6 (s)	ν_2 OD stretch of $HDSO_4$
2631.4 (s)	ν_9(b) antisymmetric OD stretch D_2SO_4
1447.9	ν_3 S=O_2 antisymmetric stretch of $HDSO_4$
1442.6 (m)	ν_{10}(b) S=O_2 antisymmetric stretch of D_2SO_4
1217.7 (s)	ν_4, ν_2(a) symmetric O=S=O stretch of $HDSO_4$/D_2SO_4
1148 (w)	ν_5 S–OH bend of $HDSO_4$?
903.7 (w)	ν_{11}(b) antisymmetric S–OD bend of D_2SO_4
887.3 (s)	ν_6 antisymmetric S–$(OH)_2$ stretch of $HDSO_4$
877.0 (s)	ν_{12}(b) antisymmetric S–$(OH)_2$ stretch of D_2SO_4
862 (vw)	ν_7 S–(OD) bend of $HDSO_4$
854 (vw)	ν_3(a) symmetric S–(OD) bend of D_2SO_4
838.8 (m)	ν_8 symmetric S–$(OH)_2$ stretch of $HDSO_4$
829.2 (m)	ν_4(a) symmetric S–$(OH)_2$ stretch of D_2SO_4
556.4 (s)	ν_9 S=O_2 rock of $HDSO_4$
554.9 (s)	ν_{13}(b) S=O_2 rock of D_2SO_4
546.0 (s)	ν_{10} S=O_2 bend of $HDSO_4$
542.9 (m)	ν_5(a) S=O_2 bend of D_2SO_4
481 (m)	ν_{11} O–S=O wag of $HDSO_4$
467.5 (m)	ν_{14}(b) O–S=O wag of D_2SO_4
267.5 (m)	ν_{14} OH torsion of $HDSO_4$
208 (w)	ν_8(a) symmetric OD torsion of D_2SO_4
187.4 (m)	ν_{15} OD torsion of $HDSO_4$

Table 4
Observed and calculated fundamental vibrations of H_2SO_4 and of D_2SO_4 (cm^{-1}) (abbreviations: s, strong; m, medium; w, weak; v, very)

		H_2SO_4						D_2SO_4			
		Vapor[a]	O_2 matrix[b]	Ne matrix[c]	Ar matrix[d]	Calculated[e]	PED[f]	Vapor[a]	Ar matrix[d]	Calculated	PED
a	ν_1				3563 (w)	3596(15)	$100S_1$			2617	$100S_1$
	ν_2	1223	1218.6	1222.0	1216.1 (s)	1212(9)	$80S_2$	1223	1217.7(s)	1212	$81S_2$
	ν_3	1138		1134.2	1135.9(w)	1139(1)	$97S_3$		854(vw)	852	$81S_3 + 16S_4$
	ν_4	834	842	835.2	831.4(m)	832(3)	$75S_4$	834	829.2(m)	826	$68S_4 + 20S_5$
	ν_5	550			548.1 (s)	548(8)	$79S_5 + 19S_7$	547	542.9(m)	543	$78S_5 + 19S_7$
	ν_6				421.7 (w)[g]	426(7)	$42S_6 + 32S_7 + 15S_5$			403	$52S_7 + 23S_5 + 20S_6$
	ν_7				378.5 (w)[g]	382(4)	$68S_7 + 25S_5$			376	$62S_7 + 21S_5 + 15S_6$
	ν_8				224 (m)[g]	226(20)	$58S_8 + 22S_6$			166	$68S_8 + 17S_6$
b	ν_9	3610	3591.6	3603.3	3566.7 (vs)	3592(56)	$100S_9$	2663	2631.8(s)	2614	$100S_9$
	ν_{10}	1450	1452.0	1461.2	1452.4 (vs)	1458(14)	$86S_{10}$	1446	1442.6(s)	1446	$92S_{10}$
	ν_{11}	1159		1156.4	1156.9 (w)	1155(15)	$87S_{11}$	820	903.7(w)	901	$64S_{11} + 26S_{12}$
	ν_{12}	883	884.6	887.3	881.7 (vs)	888(24)	$81S_{12} + 16S_{13}$	883	877(s)	881	$70S_{12} + 19S_{13}$
	ν_{13}	568	560		558.0 (s)	558(48)	$91S_{13}$	565	554.9(s)	555	$90S_{13}$
	ν_{14}				506 (m)[g]	499(37)	$87S_{14}$		467.5(m)	462	$77S_{14} + 22S_{11}$
	ν_{15}				287.7 (m)[g]	288(10)	$91S_{15}$		208(w)	213	$93S_{15}$

[a] Vapor phase data from Refs. [2–6].
[b] O_2 matrix data from Ref. [15].
[c] Ne data from Ref. [14].
[d] This work.
[e] Calculated infrared intensities $/10^{-18}$ cm per molecule given in parentheses.
[f] PED, Potential energy distribution; contributions less than 15% have been omitted. See Table 2 for definition of the symmetry coordinates.
[g] Not previously reported by us in Ref. [16].

Table 5
Observed and calculated frequencies of $HDSO_4$ fundamental vibrations (cm^{-1})

Mode	Ar matrix	Calculated	PED
ν_1	3569.1 (s)	3594	$100S_1$
ν_2	2634.6 (s)	2615	$100S_9$
ν_3	1447.9 (s)	1452	$89S_{10}$
ν_4	1217.7 ? (s)	1212	$80S_2$
ν_5	1148 (w)	1148	$91S_3$
ν_6	887.3 (s)	889	$71S_{12} + 15S_{11}$
ν_7	862 (vw)	871	$72S_{11}$
ν_8	838.8 (m)	830	$74S_4 + 16S_5$
ν_9	556.4 (s)	557	$84S_{13}$
ν_{10}	546.0 (s)	546	$79S_5 + 19S_7$
ν_{11}	481	482	$80S_{14}$
ν_{12}		413	$38S_7 + 32S_6 + 18S_5$
ν_{13}		379	$67S_7 + 24S_5$
ν_{14}	267.5 (m)	265	$72S_8$
ν_{15}	187.4 (m)	180	$65S_{15} + 16S_6$

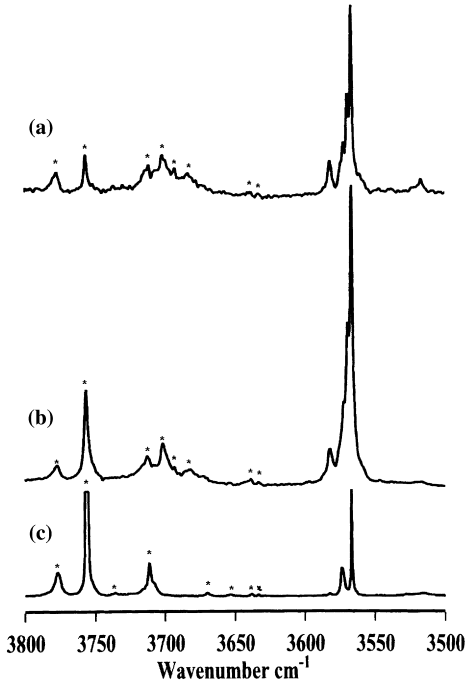

Fig. 2. OH stretch mode region of sulfuric acid vapors trapped in argon at 5 K (*, bands of water only species): (A) H_2SO_4 vapors; (B) D_2SO_4 vapors; and (C) sample B temperature cycled to 25 K.

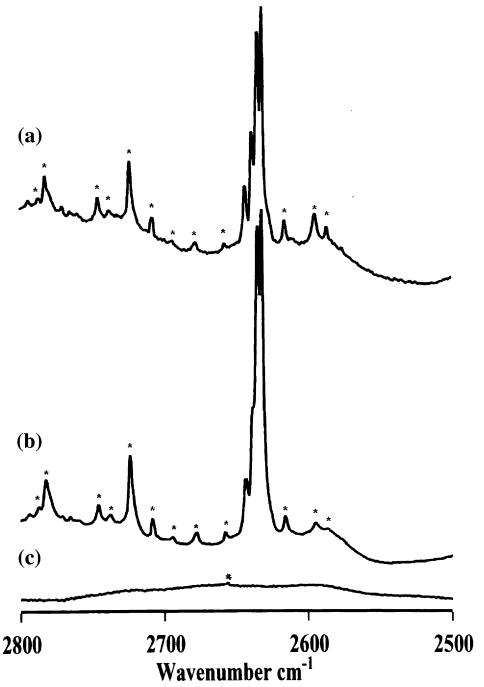

Fig. 3. OD stretch mode region of sulfuric acid vapors trapped in argon at 5 K (*, bands of water only species): (A) H_2SO_4 vapors; (B) D_2SO_4 vapors; and (C) sample B temperature cycled to 25 K.

3.4.1. OH stretch region

This region, reproduced in Fig. 2, reveals several bands belonging to rotating and non-rotating monomers and polymers of H_2O (3776, 3756, 3711, 3707, 3670, 3653, 3638, 3633 and 3517 cm^{-1}, traces A, B and C) and HDO species (3701.7, 3699, 3693 and 3682 cm^{-1}, traces B and C) [35–37]. Trace A contains, in addition, a strong sharp band at 3566.7(1.1) cm^{-1}, assigned to the ν_9(b) mode of H_2SO_4, accompanied by two lines at 3572.6(1) and 3582(2.8) cm^{-1}, assigned to $(H_2O)\cdot(H_2SO_4)$ and $(H_2O)_2\cdot(H_2SO_4)$, respectively [16]. In the corresponding region of the D_2SO_4 sample (trace B), an additional band at 3569.1 cm^{-1} is recorded and assigned to the ν_1 OH stretch of $HDSO_4$. A shift towards higher wave numbers (2.4 cm^{-1}) by isotopic substitution of hydrogen by deuterium may seem rather unusual. However, our ab initio calculations (Table 4) also indicate the $HDSO_4$ band to be 2 cm^{-1} higher than the H_2SO_4 antisymmetric stretch and to have about a quarter of its intensity.

For H_2SO_4, the two OH stretching vibrations are

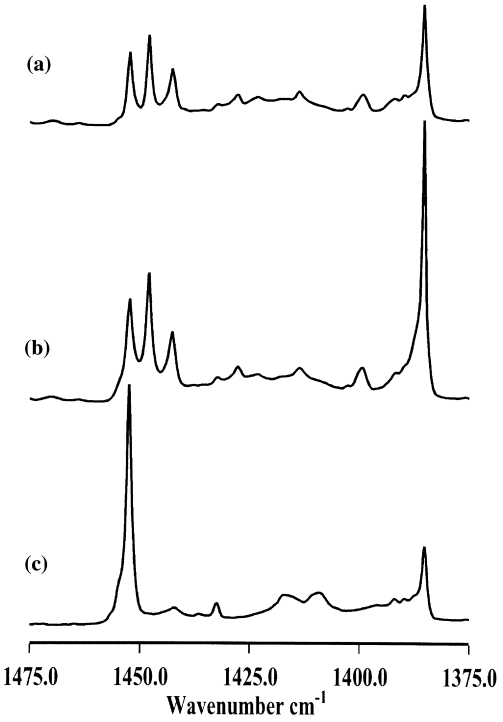

Fig. 4. S=O_2 antisymmetric stretch mode region of sulfuric acid vapors trapped in argon at 5 K: (A) H_2SO_4 vapors; (B) D_2SO_4 vapors; and (C) sample B temperature cycled to 25 K.

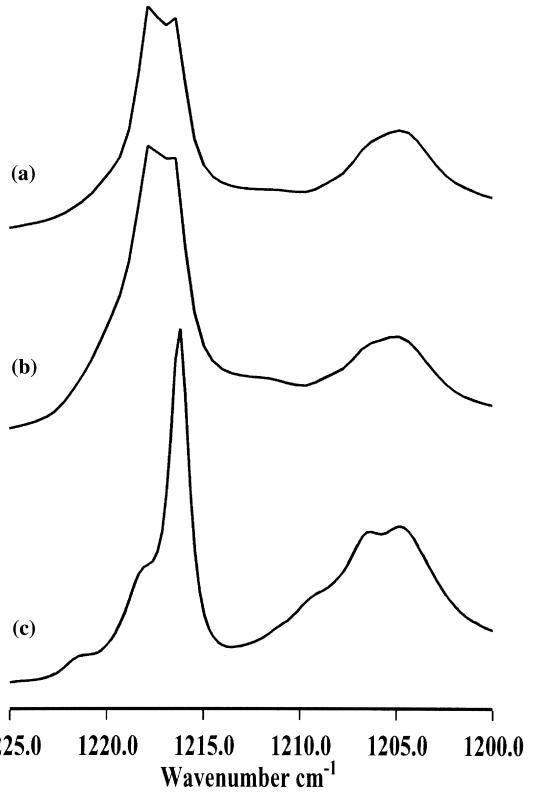

Fig. 5. S=O_2 symmetric stretch mode region of sulfuric acid vapors trapped in argon at 5 K: (A) H_2SO_4 vapors; (B) D_2SO_4 vapors; and (C) sample B temperature cycled to 25 K.

almost completely uncoupled as they do not involve a common atom. In our previous study [16] we assigned the ν_1(a) of H_2SO_4 to a weak band at 3563 cm^{-1}. Our present calculations (Table 4) predict the ν_1(a) band of H_2SO_4 to be a few wave numbers higher than that of the antisymmetric ν_9(b) stretch and to have over 20% of the intensity of the latter. However, this spectral region is obscured by the two rather strong bands of the $(H_2O)_2$ dimer and the antisymmetric stretch of the $(H_2O)\cdot(H_2SO_4)$ complex [16]. No spectral evidence points to the 3572.6 cm^{-1} composite band having an additional third component of significant intensity, unaffected by temperature cycling and hence assignable to the ν_1(a) mode. We, therefore, revert to our original assignment [16] of this mode to the weak band at 3563 cm^{-1}. Even though its position is to the low energy side of its antisymmetric counterpart, and its intensity is lower than that predicted by the calculation, the most relevant attribute, the behavior with temperature cycling, is in accord with the suggested assignment.

No new features appear as a result of deuteration, next to the $(H_2O)\cdot(H_2SO_4)$ absorptions mentioned above. This indicates that the interaction of H_2O, HDO and D_2O with H_2SO_4 is essentially unaffected by deuteration, and hence involves the water oxygen and the acid hydrogen [16], a bonding scheme supported by recent ab initio calculations [38,39]. The complexation of H_2SO_4 with H_2O is a minimum energy process [38]. Taking the experimental values for the ν_9(b) asymmetric stretch, the ab initio calculation predicts the position of the H-bonded OH stretch of the $(H_2O)\cdot(H_2SO_4)$ complex to be shifted -560 cm^{-1} from that of the free H_2SO_4 molecule [38]. No band with the required intensity dependence on temperature cycling or water concentration is found in the suggested region. However, as noted above, the band assigned by us to this mode at 3572.6 cm^{-1} shows this characteristic quite

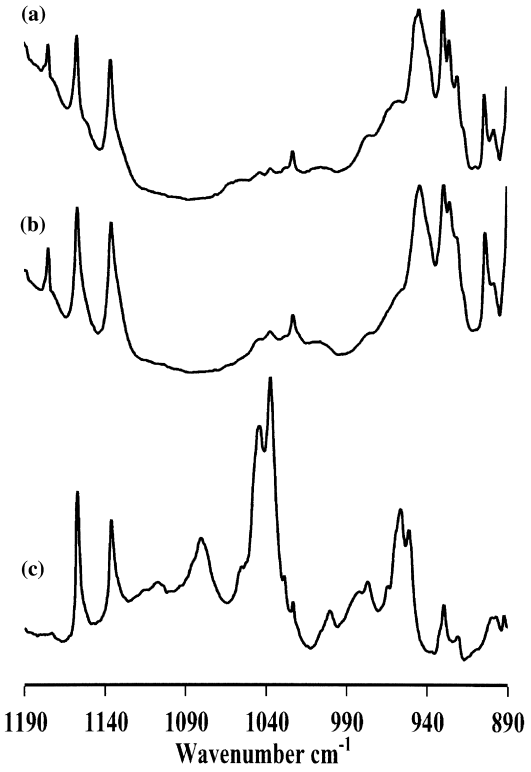

Fig. 6. S–$(OH)_2$ bend modes region of sulfuric acid vapors trapped in argon at 5 K: (A) H_2SO_4 vapors; (B) D_2SO_4 vapors; and (C) sample B temperature cycled to 25 K.

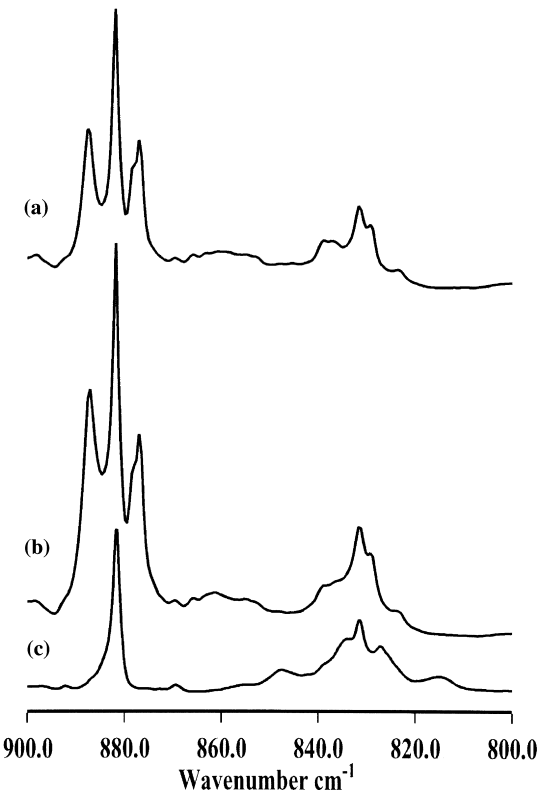

Fig. 7. S–$(OH)_2$ stretching modes region of sulfuric acid vapors trapped in argon at 5 K: (A) H_2SO_4 vapors; (B) D_2SO_4 vapors; and (C) sample B temperature cycled to 25 K.

prominently. It is, admittedly, surprising to observe the 1:1 water complex of H_2SO_4 to be not shifted to the red and even appear at a higher energy position than the free acid molecule. A possible explanation is that one of the water hydrogens interacts with the non-bonding electrons of the acid OH oxygen, thus making a compensating bond strengthening contribution (rather than a weak interaction with the double bonded S=O oxygen, as suggested by Beichert et al. [38]).

3.4.2. OD stretch region

The OD stretching region, reproduced in Fig. 3, reveals a pattern similar to that observed in the OH stretch region. The spectral bands comprise several D_2O and HDO monomeric and polymeric absorptions [35–37], e.g. at (2782.2, 2770.3, 2745.7, 2723.6, 2707.6, 2677.7, 2657.6, 2615.8, 2594.8 and 2586.5 cm^{-1}). Four additional lines are observed in this region. Of the latter, the two strong bands at 2631.4(1.2) and 2634.6(1.8) cm^{-1} (Fig. 3, trace B) are readily assigned to the antisymmetric OD stretch ν_9(b) mode of D_2SO_4 and the ν_2 OD stretch of $HDSO_4$ respectively. Similar to the OH stretch region, the OD stretch frequency in $HDSO_4$ appears slightly (3.2 cm^{-1}) higher than the ν_9(b) mode in D_2SO_4. The medium intensity absorptions at 2638.5(2) cm^{-1} which includes a contribution from the 2639 cm^{-1} $(HDO)_2$ band and at 2643.2(2.1) cm^{-1} are not observed in either the argon matrix H_2SO_4 (Trace A) or D_2O spectrum [35–37] and are therefore attributed to D_2SO_4 and $HDSO_4$ containing species. As these bands readily increase upon temperature cycling (Fig. 3, trace C), it indicates the involvement of water species in their origin. The strong resemblance to the OH stretching region in the quartet structure, in the relative intensities and in temperature cycling behavior, supports the assignment of the 2638.5 and

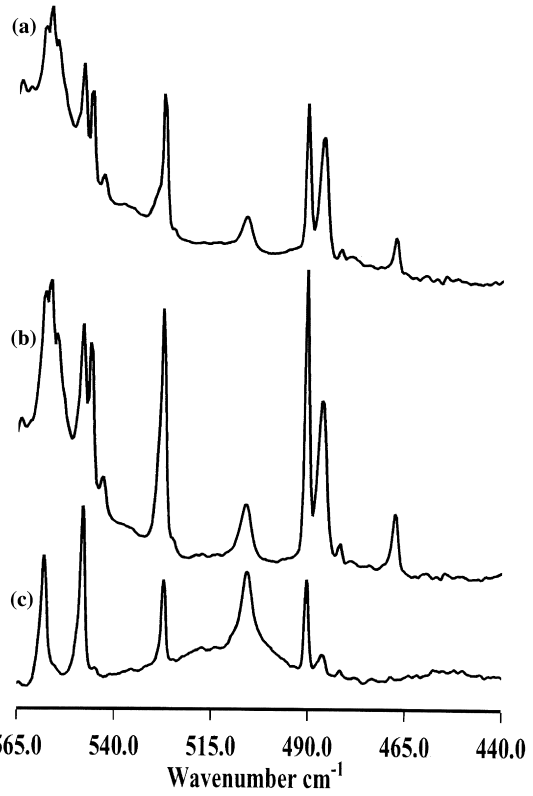

Fig. 8. S=O_2 rock and bend modes region of sulfuric acid vapors trapped in argon at 5 K: (A) H_2SO_4 vapors; (B) D_2SO_4 vapors; and (C) sample B temperature cycled to 25 K.

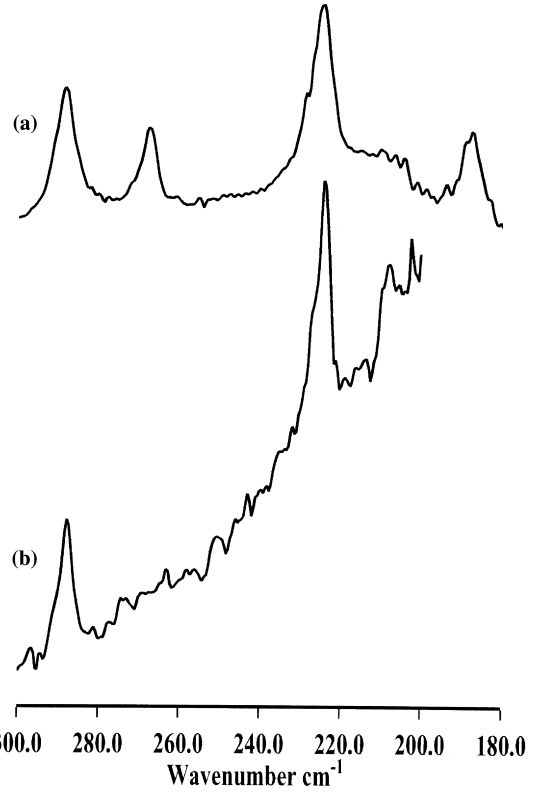

Fig. 9. Far-infrared torsional modes region of sulfuric acid vapors trapped in argon at 5 K: (A) H_2SO_4 vapors; and (B) D_2SO_4 vapors.

2643.2 cm^{-1} bands to complexes of partially or fully deuterated sulfuric acid with partially or fully deuterated water momomers, $(D_2O/HDO)\cdot(D_2SO_4/HDSO_4)$, and dimers $((D_2O)_2/(HDO)_2)\cdot(D_2SO_4/HDSO_4)$, respectively. The almost identical isotope effect (1.3540–1.3554) observed for all four bands is another evidence for their common origin—the sulfuric acid OH and OD stretches.

3.4.3. S=O_2 stretch region

This spectral region also includes several bands attributed to the ν_2 bend modes of rotating and non-rotating HDO monomers and to $(HDO)_2$ at 1432.2, 1427.7, 1413.9, and 1399.1 cm^{-1} (Fig. 4). The isotopic pattern observed in the antisymmetric O=S=O stretching region, Fig. 4, is particularly pleasing. The antisymmetric O=S=O stretching mode is calculated as one of the strongest IR bands (Table 4), and the assignment of the bands at 1452.4(1.4), 1447.9(1.2), and 1442.6(1.5) cm^{-1} to this mode in H_2SO_4, $HDSO_4$, and D_2SO_4 is straightforward. It may be noted that the relative band intensities roughly correspond to a H_2SO_4:D_2SO_4:$HDSO_4$ composition of 1:1:1 for the sample shown. This normal mode consists of 86% (H_2SO_4), 89% ($HDSO_4$) and 92% (D_2SO_4) of the O=S=O stretching coordinate (Tables 2 and 4) a fact which is well reflected in the small ν_{OH}/ν_{OD} isotope effect.

This is further accentuated in the symmetric O=S=O stretching mode isotope effect (Fig. 5) where the bands of the three isotopomers overlap almost completely. In the parent H compound the ν_2(a) band appears as a strong, sharp band at 1216.1(1) cm^{-1}. In the spectrum of the mixed isotopes the 1216.5(1) cm^{-1} is a shoulder on the stronger 1217.7(1) cm^{-1} band, which is apparently a superposition of both the D_2SO_4 and $HDSO_4$ components.

In contrast to the antisymmetric O=S=O stretching mode the symmetric O=S=O stretching mode in $HDSO_4$ and D_2SO_4 is located at higher wave numbers than in H_2SO_4. The calculated harmonic frequencies for the symmetric O=S=O stretch are not at all affected by deuteration (Table 4). As there are no neighboring bands which could account for a possible resonance, the observed small shifts may then be due to anharmonic cross terms with modes involving the hydrogens.

3.4.4. S–OH bend modes

The two S–O–H bend modes, ν_3(a) and ν_{11}(b) in H_2SO_4 are assigned to the medium intensity bands at 1135.9(5.9) and 1156.9(3.5) cm^{-1}, respectively (Fig. 6, trace A). This vibrational mode is sensitive to the molecular environment, almost as much as the OH stretch mode. This is well demonstrated by the wave number values in a CO matrix, 1267.6 and 1229.5 cm^{-1} [23] as compared to the crystalline phase values, 1240 and 1170 cm^{-1} [13]. In the matrix spectrum of the deuterated sample (Fig. 6, trace B) two additional weak bands at 1195.2 and 1174.9 cm^{-1} belong to the ν_2 bend modes of D_2O species [35–37]. For $HDSO_4$ the S–O–H bend mode is expected at the average wave number of the two H_2SO_4 bands, with half their individual intensity. The calculation places it at 1147 cm^{-1} (Table 5). Only a weak indication of a band is observed around 1148 cm^{-1} and hence its assignment to ν_5 of $HDSO_4$ is somewhat tentative.

Examination of the low wave number range of the OH bands (Fig. 6, trace B) shows several absorptions (950, 929, 920 cm^{-1}) previously assigned to $(H_2O)_m{\cdot}(H_2SO_4)_n$ and $(H_2O)_m{\cdot}(H_2SO_4)_n{\cdot}(SO_3)_p$ polymers [16], and a clear new weak band at 903.7 cm^{-1}, assigned to ν_{11}(b) of D_2SO_4, in good accord with the calculated value of 901 cm^{-1} (Table 4). The lower energy symmetric bend modes of the deuterated acids coincide with the much stronger bands of the S–O stretch modes. Only after spectral subtraction two weak features are discerned at 862 and 854 cm^{-1}. Relying on the calculated values for D_2SO_4 and $HDSO_4$ at 852 and 869 cm^{-1}, respectively, and in view of the lack of more pronounced features, we boldly assign these features to the ν_3(a) mode of D_2SO_4 and the ν_7 mode of $HDSO_4$.

For comparison, the gas phase value of for the ν_3(a) mode for D_2SO_4 is 820 cm^{-1} [2] and the crystal value for the antisymmetric ν_{11}(b) mode is 930 cm^{-1} [7]. The isotope effect for the antisymmetric ν_{11}(b) mode is 1.273 and for the tentatively assigned symmetric ν_3(a) mode it is 1.33. This rather large effect (about 0.93 of the effect in the OH/OD stretch) is further support of the assignment.

3.4.5. S–OH stretching modes

These two modes are essentially S–O stretches (Tables 2 and 4), so that the isotope effect expected and observed here is very small. Fig. 7 shows the isotopic splitting of the two modes. The 881.7(1.3) cm^{-1} antisymmetric stretch absorption of H_2SO_4 is thus enclosed by the 887.3(2.2) cm^{-1} $HDSO_4$ and the 877(2.4) cm^{-1} D_2SO_4 bands, whereas the 831.4 cm^{-1} H_2SO_4 symmetric stretch line is accompanied by the 838.8 cm^{-1} $HDSO_4$ and the 829.2 cm^{-1} D_2SO_4 bands. These observed band positions are very close to the ab initio calculated values (Table 4).

3.4.6. S=O_2 rock and bend modes

These two modes, ν_5(a) and ν_{13}(b) appear at 548.1(1.3) and 558(1) cm^{-1}, respectively, in the argon isolated H_2SO_4 infrared spectrum [16]. They are not expected to show any large isotope effects. As shown in Fig. 8 (traces A and B), the relevant $HDSO_4$ and D_2SO_4 bands (ν_{10} and ν_5(a), respectively) emerge at 546(1) and 542.9(1.1) cm^{-1}, and at 556.4(1) and 554.9(1) cm^{-1} (ν_9 and ν_{13}(a), respectively). These frequencies agree very well with the calculated values (Tables 4 and 5) and their very small H/D isotope effect is similar to those of other O=S=O and S–OH motions.

3.4.7. Far-infrared bands

The intensity of the broad 506(3.5) cm^{-1} band was shown by us [16] to depend upon both water and sulfuric acid concentrations, leading to its assignment to polymeric $(H_2O)_m{\cdot}(H_2SO_4)_n$ species. However, in later experiments, with nitrogen mixed in various amounts into the argon matrix [24], this band also demonstrated monomeric characteristics—shifting with the other H_2SO_4 fundamentals. Our ab initio calculations predict the ν_{14}(b) O–S=O wagging to be located around 500 cm^{-1} with its D_2SO_4 counterpart around 460 cm^{-1}. In our "D_2SO_4" vapor spectrum (Fig. 8, trace B) a new band is found at

Table 6
Thermodynamic properties of H_2SO_4

T (K)	C_p (J/(K mol))	C_p/C_v	S (J/(K mol))	$H - H_0$ (kJ/mol)	$-(G - H_0)/T$ (J/(K mol))
100	41.8	1.248	290.17	3.53	254.95
150	53.35	1.185	309.27	5.91	269.99
200	64.51	1.148	326.18	8.86	281.99
250	74.4	1.126	341.66	12.34	292.41
273.16	78.57	1.118	348.43	14.11	296.89
298.16	82.78	1.112	355.5	16.13	301.52
300	83.08	1.111	356.01	16.28	301.85
350	90.65	1.101	369.4	20.63	310.57
400	97.2	1.094	381.94	25.33	318.73
450	102.83	1.088	393.72	30.33	326.43
500	107.65	1.084	404.81	35.6	333.73
550	111.79	1.08	415.27	41.09	340.68
600	115.36	1.078	425.16	46.77	347.32
650	118.46	1.075	434.52	52.61	353.68
700	121.18	1.074	443.4	58.61	359.78
750	123.59	1.072	451.84	64.73	365.64
800	125.75	1.071	459.89	70.96	371.29
850	127.69	1.07	467.57	77.3	376.74
900	129.46	1.069	474.92	83.73	382
950	131.07	1.068	481.96	90.24	387.08
1000	132.56	1.067	488.72	96.83	392

467.5(1.7) cm^{-1}. We, therefore assign the 506 cm^{-1}, in part, and 467.5 cm^{-1} bands to the ν_{14}(b) modes of H_2SO_4 and D_2SO_4 monomers, respectively. The corresponding mode (ν_{11}) in $HDSO_4$ is predicted around 480 cm^{-1} and may overlap the 481 cm^{-1} band originating from SO_3 perturbed by H_2O [16]. We indeed note that in the "D_2SO_4" experiments this band attains higher relative intensities.

Two additional weak bands were discerned—a broad band centered at 421.7(10) cm^{-1} and a very weak broad band at 378.5(12) cm^{-1}. Their positions resemble the calculated values for the weak ν_6(a) and ν_7(a) modes around 430 and 380 cm^{-1}, respectively. These vibrational modes are essentially O–S=O bending modes (Tables 2 and 4) with no significant changes in bond lengths during the motion. The dipole moment changes are affected only through variations in the S–OH bond direction, leading to the low observed and calculated intensities. The band positions are not affected much by deuteration, in accord with the ab initio calculations (Table 4).

3.4.8. Torsional modes bands

In the even lower energy torsional modes region of H_2SO_4 (Fig. 9, trace A), two medium intensity bands were recorded at 287.7(3.5) and 224(3.4) cm^{-1}. They are assigned to the ν_{15}(b) antisymmetric and to the ν_8(a) symmetric O=S–O–H torsion modes, in remarkable agreement with the calculated frequencies (Table 4). A previous calculation yielded harmonic values of 280 and 265 cm^{-1}, respectively [29]. The average of the experimental values—255.8 cm^{-1}, is close to the gas phase torsion of the single OH mode of HSO_3F [7]. The parallel spectrum of the D_2SO_4 vapors (Fig. 9, trace B) shows two additional medium intensity bands at 267.5(4.4) and 187.4(6.2) cm^{-1}, along with a weak band at 208(3.4) cm^{-1}. We assign the 267.5 cm^{-1} band to the OH torsion of $HDSO_4$, the 187.4 cm^{-1} to the OD torsion of the same species and the 208 cm^{-1} feature to the antisymmetric O=S–O–D torsion of D_2SO_4.

3.4.9. SO_3 bands

The spectra of "D_2SO_4" vapors demonstrate the three monomeric SO_3 fundamental bands at 1385.1(1), 527.2 (1.7) and 490.3(1.1) cm^{-1}, three bands at 1389 and 481 cm^{-1} of dimeric $(SO_3)_2$ and a 486.2 cm^{-1} feature attributed to SO_3 monomers perturbed by H_2O neighbors [16]. No new bands could be attributed to the influence of D_2O or HDO

on the SO_3 species. This is further support for our argument that no stabilization of $(H_2O)_m \cdot (SO_3)_n$ species occurs in argon matrices [16].

3.4.10. Fundamental modes of vibration—summary

The far infrared spectra and ab initio calculations enabled us to assign *all* 15 normal modes of the H_2SO_4 argon isolated monomer for the first time. In the comparison between calculated and experimental vibrational frequencies, it should be remembered that the latter are recorded of an argon matrix which tends to shift the vibrational modes to lower energies ('matrix shift'). As the basic calculations involve 'harmonic' frequencies, this may tend to increase the difference between theoretical and observed values, especially for the angle bend and deformation modes, which are intrinsically of highly anharmonic nature. Experimental reasons limited our studies to above 180 cm^{-1}, which, in addition to the low intensity expected for the low lying deformation mode bands (cf. calculation results in Tables 4 and 5), prevented the experimental observation of all the vibrational frequencies for all three isotopic species.

3.5. Thermodynamic properties

With all 15 normal vibrations of monomeric H_2SO_4 assigned and a set of calculated coordinates available for the minimum energy configuration, it is possible to evaluate its "ideal gas" thermodynamic properties. These are summarized in Table 6 for the temperature range of 100–1000 K.

Acknowledgements

This work has received support from The Research Council of Norway (Programme for supercomputing) through a grant of computing time. A.L. acknowledges a visiting scientist scholarship from the Research Council of Norway.

References

[1] A. Jaecker-Voirol, P. Mirabel, H. Reiss, J. Chem. Phys. 87 (1987) 4849.
[2] S.M. Chakcalackal, F.E. Stafford, J. Am. Chem. Soc. 88 (1966) 723.
[3] K. Stopperka, F. Kilz, Z. Anorg. Allg. Chem. 370 (1969) 49.
[4] K. Stopperka, F. Kilz, Z. Anorg. Allg. Chem. 370 (1969) 59.
[5] R.F. Majkowski, R.J. Blint, J.C. Hill, Appl. Opt. 17 (1978) 975.
[6] R.S. Eng, G. Petagana, K.W. Nill, Appl. Opt. 11 (1978) 1723.
[7] P.A. Giguere, R. Savoie, Can. J. Chem. 38 (1960) 2467.
[8] G.E. Walrafen, D.M. Dodd, Trans. Faraday Soc. 57 (1961) 1286.
[9] R.J. Gillespie, E.A. Robinson, Can. J. Chem. 40 (1962) 644.
[10] P.A. Giguere, R. Savoie, J. Am. Chem. Soc. 85 (1963) 287.
[11] K. Stopperka, F. Kilz, Z. Anorg. Allg. Chem. 370 (1969) 80.
[12] C.E.L. Myhre, Cand. Scient. Thesis, University of Oslo, 1996.
[13] A. Gopyron, J.D. Villepin, A. Novak, Spectrochim. Acta 31A (1975) 805.
[14] V.E. Bondybey, E. English, J. Mol. Spectrosc. 109 (1985) 221.
[15] T.L. Tso, E.K.C. Lee, J. Phys. Chem. 88 (1984) 2776.
[16] A. Givan, L.A. Larsen, A. Loewenschuss, C.J. Nielsen, J. Chem. Soc. Faraday Trans. 94 (1998) 827.
[17] L. Schriver, D. Carrere, A. Schriver, K. Jaeger, Chem. Phys. Lett. 181 (1991) 505.
[18] M. Hoffman, P.R. Schleyer, J. Am. Chem. Soc. 116 (1994) 494.
[19] A.W. Castleman, R.E. Davis, H.R. Munkelwitz, I.N. Tang, W.P. Wood, Int. J. Chem. Kinet. Symp. 1 (1975) 629.
[20] T.S. Chen, P.L.M. Plummer, J. Phys. Chem. 89 (1985) 2231.
[21] K. Morokuma, C. Muguruma, J. Am. Chem. Soc. 116 (1994) 10 316.
[22] C.E. Kolb, J.T. Jayne, D.R. Worsnop, M.J. Molina, R.F. Meads, A.A. Viggiano, J. Am. Chem. Soc. 116 (1994) 10 314.
[23] A. Givan, L.A. Larsen, A. Loewenschuss, C.J. Nielsen, J. Chem. Soc. Faraday Trans. 94 (1998) 2227.
[24] A. Givan, A. Loewenschuss, C.J. Nielsen, Phys. Chem.: Chem. Phys. 1 (1999) 37.
[25] A. Givan, A. Loewenschuss, C.J. Nielsen, submitted for publication.
[26] A. Givan, A. Loewenschuss, C.J. Nielsen, submitted for publication.
[27] E. Kemnitz, C. Werner, S. Trojanov, Acta Crystallogr. C52 (1996) 2665.
[28] R.L. Kuczkowski, R.D. Suenram, F.J. Lovas, J. Am. Chem. Soc. 103 (1981) 2561.
[29] L.L. Lohr Jr., J. Mol. Struct. 87 (1982) 221.
[30] P. Kaliannan, S. Vishveshwara, V.S.R. Rao, J. Mol. Struct. 92 (1983) 7.
[31] M. Hofmann, P. von Ragué Schleyer, J. Am. Chem. Soc. 116 (1994) 4947.
[32] G.P. Ayers, R.W. Gillett, J.L. Gras, Geophys. Res. Lett. 17 (1980) 433.
[33] J.I. Gmitro, T. Vermeulen, AIChE J. 10 (1964) 740.
[34] M.J. Frisch, G.W. Trucks, H.B. Schlegel, P.M.W. Gill, B.G. Johnson, M.A. Robb, J.R. Cheeseman, T. Keith, G.A. Petersson, J.A. Montgomery, K. Raghavachari, M.A. Al-Laham, V.G. Zakrzewski, J.V. Ortiz, J.B. Foresman, J. Cioslowski, B.B. Stefanov, A. Nanayakkara, M. Challacombe, C.Y. Peng, P.Y. Ayala, W. Chen, M.W. Wong, J.L. Andres, E.S. Replogle, R. Gomperts, R.L. Martin, D.J. Fox, J.S.

Binkley, D.J. Defrees, J. Baker, J.P. Stewart, M. Head-Gordon, C. Gonzalez, J.A. Pople, Gaussian 94, Revision D.2, Gaussian, Inc., Pittsburgh PA, 1995.
[35] R.M. Bentwood, A.J. Barnes, W.J. Orville-Thomas, Molec. Spectrosc. 84 (1980) 391.
[36] G.P. Ayers, A.D.E. Pullin, Spectrochim. Acta 32A (1976) 1629.
[37] G.P. Ayers, A.D.E. Pullin, Spectrochim. Acta 32A (1976) 1641.
[38] P. Beichert, O. Schrems, J. Phys. Chem. 102A (1998) 10540.
[39] H. Arsila, K. Laasonen, A. Laaksonen, J. Chem. Phys. 108 (1998) 1031.